Organic & Biomolecular Chemistry

ROYAL SOCIETY OF CHEMISTRY

PAPER

View Article Online
View Journal

Open Access Article. Published on 05 January 2026. Downloaded on 1/11/2026 12:59:57 PM.
This article is licensed under a Creative Commons Attribution-NonCommercial 3.0 Unported Licence.

Check for updates

Cite this: DOI: 10.1039/d5ob01455g

A computational investigation of the thermal elimination chemistry of β-borylated sulfoxides. Sulfenic acid *vs.* boryl sulfenate elimination

Eric A. Nicol and Adrian L. Schwan *

Received 10th September 2025,
Accepted 19th December 2025

DOI: 10.1039/d5ob01455g

rsc.li/obc

Electronic structure calculations were performed to assess how a β-boryl substituent modulates barriers for the classical Ei elimination of sulfoxides. Four main boron substituents were investigated: H, Me, F and OMe. Across the series, methanesulfenic-acid elimination exhibits reduced activation free energies and enthalpies as the boron functionality accepts electron density from the C_β–H bond, promoting a more asynchronous transition state with advanced C_β–H cleavage and O–H formation and correspondingly less S–C_α bond rupture relative to the benchmark ethyl methyl sulfoxide transition state. Nevertheless, β-boryl substrates of the **1B** family access lower-energy minima that lead preferentially to boryl sulfenate elimination: the corresponding $\Delta G^\ddagger$ values are 9.5–15.5 kcal mol^{-1} lower than for the competing proton-transfer (sulfenic-acid) pathway. Replacing methyl with vinyl or phenyl lowers $\Delta G^\ddagger$ by 1.9–4.9 kcal mol^{-1} through enhanced stabilization of developing electron density at sulfur. A comparison of common boronic esters (catechol, pinacol, BMIDA) for both proton-transfer and boronic-ester-transfer pathways shows catechol (**Bcat**) gives the lowest barriers, whereas BMIDA is distinctive in that its methanesulfenic acid elimination resembles that of methyl ethyl sulfoxide, and boryl-sulfenate elimination is disfavoured owing to loss of intramolecular N → B coordination. Collectively, β-boryl substitution lowers Ei barriers *via* electron-acceptor stabilization and biases reaction manifolds toward boryl sulfenate elimination, with the extent governed by conjugation patterns and ester identity.

Introduction

For more than 50 years,[1–3] the thermal *syn* elimination of sulfenic acid from an organic molecule possessing a sulfoxide and a vicinal hydrogen (Fig. 1a) has been a staple in organic synthesis. This reaction places a double bond between carbons that held a sulfoxide and β-hydrogen of suitable positioning and has been an important step in numerous synthetic sequences.[4–8] The reaction has also found applications in materials[9] and polymer[10] chemistries and as a source of slow-release fragrances.[11]

Known to proceed by an internal elimination (Ei) mechanism,[12,13] the elimination has been explored extensively by the Barattucci/Bonaccorsi group with a focus on transforming the sulfenic acid fragment,[14–16] to create (a) a series of mixed disulfides with applications to linker technology and nanoparticle formation and (b) a collection of sulfoxides with applications as ligands, sulfinyl dienes, bolaamphiphiles and bioactive glycoconjugates.

Department of Chemistry, University of Guelph, Guelph, ON, N1G 2W1, Canada. E-mail: schwan@uoguelph.ca

Among the computational studies of the reaction,[13,17–19] the Jenks group[13] performed an extensive study of the elimination reaction through a combined theoretical and experimental analysis of over 31 compounds (Fig. 1b).[13] Those researchers synthesized and performed the elimination on 12 of the 31 sulfinyl compounds explored computationally.

The simplest structures proceeded to eliminate with a $\Delta H^\ddagger$ barrier of 32.9 kcal mol^{-1} (Fig. 1b).[13] Conjugation to the sulfinyl group in the form of vinyl ethyl sulfoxide and phenyl ethyl sulfoxide reduced $\Delta H^\ddagger$ values by approximately 2 kcal mol^{-1}. The work also addressed many substitution and electronic effects. For example, the presence electron withdrawing groups at β-carbon could lower the enthalpy of activation by 8.1–9.8 kcal mol^{-1} whereas such a group at the α-carbon stabilized the transition state by 10–11 kcal mol^{-1}. The work of Claes,[20] further broke down the roles of carbon backbone substituents on rate and synchronicity of the Ei mechanism.[18,20,21]

Substitution or positioning of different atoms for this thermolytic reaction has been the focus of other studies,[12,22] where the sulfur can be replaced by nitrogen (Cope elimination)[12] or selenium.[22] The latter is commonly preferred over sulfur in synthetic chemistry due to the near room temperature conditions required for the elimination.[23–25] Due to reactivity

Open Access Article. Published on 05 January 2026. Downloaded on 1/11/2026 12:59:57 PM.
This article is licensed under a Creative Commons Attribution-NonCommercial 3.0 Unported Licence.

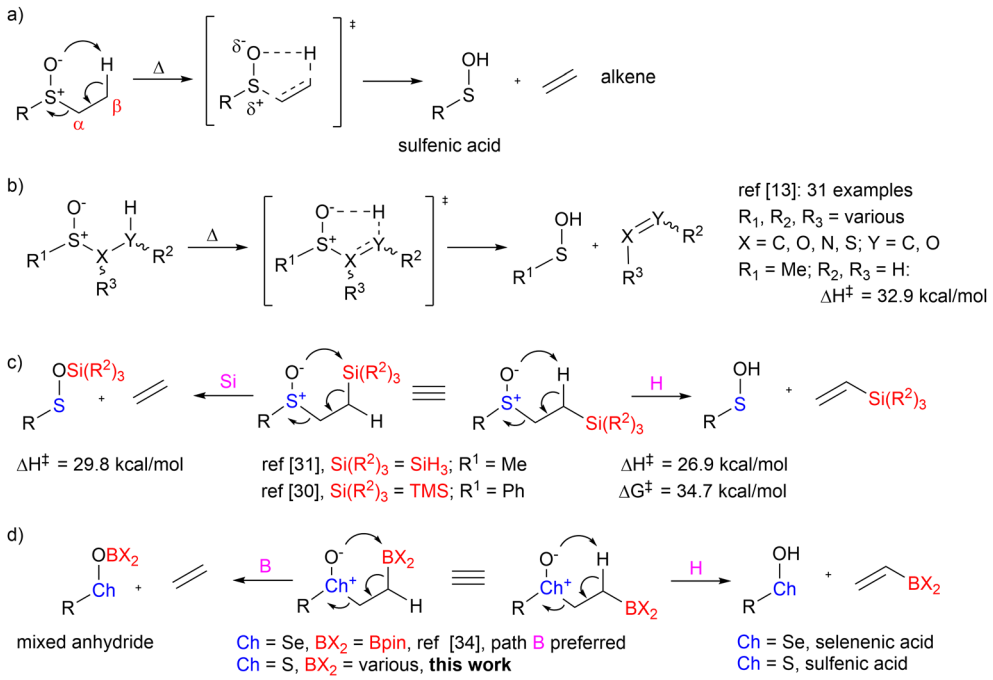

Fig. 1 Examples of eliminations of sulfenic acid derivatives.

similarities between hydrogen and silicon atoms,[26] the placement of a silicon atom β to the sulfur has the potential to create a competitive option for the sulfinyl oxygen's preferred interaction. When studied, it was determined that the silicon group activates the hydrogen on the same carbon accelerating sulfenic acid elimination (Fig. 1c)[27–30] even though the barrier for $RSOSiH_3$ elimination falls below 32.9 kcal mol^{-1}.[27–31]

Natural bond orbital (NBO) and Natural Population Analysis (NPA) showed that the silicon had the greatest effect in stabilizing the positive charge developing on C_β relative to the TMS group.[30] This work prompted McCulla and Jenks to further analyse the effects of a β-silicon on the sulfoxide elimination.[31] Employing computational protocols previously established by the Jenks group,[13] analysis was performed with SiH_3 instead of the $SiMe_3$ group for computational efficiency.[31] SiH_3 substitution at C_β reduces activation barriers, with a diminution of 10.2 kcal mol^{-1} attributed primarily to the polarizability of the silicon atom.[31]

Having computationally probed the interaction of a sulfenate oxygen with boron,[32] and realizing the influence of an electropositive silicon atom, we were interested to learn about the interaction of a sulfoxide oxygen with β-positioned boron atoms to determine the nature of the sulfinyl oxygen's engagement with the boron atom for thermal elimination chemistry. Such a reaction has already been observed between a boronate ester β to a selenoxide by the Aggarwal group who exhibited the elimination as an olefination reaction (Fig. 1d).[33,34] The study included computational work that indicated elimination would proceed with a low barrier ($\Delta G^{\ddagger}$ = 0.4–2.2 kcal mol^{-1}) through seleninyl oxygen engagement of a β-boronate ester in preference to selenenic acid loss.[34] The following work entails a computational study to evaluate similar competitive elimination chemistries of β-boryl sulfoxides and the role the boryl substituent plays in sulfenic acid elimination. The computations were performed in the gas phase to facilitate comparison to past contributions[13,34] and to permit a focus on the electronics of the interactions, as there is a paucity of literature addressing the interaction of sulfinyl oxygens with organoboron functional groups.

Computational methodology

Calculations on all structures (starting sulfoxides, transition states and products) were performed at two levels of theory. Geometry optimizations, frequency calculations, and intrinsic reaction coordinate (IRC) analyses were conducted in the gas phase at 298.15 K and 1 atm using the B3LYP functional[35–37] with the D3 dispersion correction of Stefan Grimme[38] and the def2-TZVP basis set,[39] as implemented in Gaussian 16 (Revision C.01).[40] Minima were identified by a lack of imaginary frequencies; all transition states were confirmed by the presence of a single imaginary frequency which corresponded to the atomic motion for the appropriate reaction and verified *via* IRC analysis. Single-point electronic energies were computed at the B3LYP-D3 geometries using DLPNO-CCSD(T)[41,42] with tight PNO settings and a complete basis set (CBS) extrapolation from the def2-TZVP and def2-QZVP basis sets, as implemented in ORCA 4.0.[43,44] These methods were combined to evaluate the thermodynamics of both activation and reaction processes. Natural Resonance Theory (NRT) bond orders, Natural Population Analysis (NPA) charges, second-order per-

Open Access Article. Published on 05 January 2026. Downloaded on 1/11/2026 12:59:57 PM.
This article is licensed under a Creative Commons Attribution-NonCommercial 3.0 Unported Licence.

turbation stabilization energies, and natural steric exchange energies (SXE) were obtained using NBO7.[45–47] QTAIM analysis for bond critical points were identified using AIM2000.[48] For analysis of the BMIDA systems, a global minimum structure was identified *via* the GOAT program of ORCA 6.0.[49,50] Figures were generated using CYLView[51] for general structures and AIM2000 for bond critical point images.

Results and discussion

Sulfenic acid elimination from β-boryl sulfoxides

The initial investigation was to establish the role of the geminal borane or boronate on the barriers of the Ei elimination of methanesulfenic acid from the sulfoxides, leading to the formation of a vinyl borane or boronate. Four boron substituents were investigated to determine the effect of Lewis acidity on the proton transfer reaction: H, F, Me, and OMe. Transition states for each elimination reaction were located; starting structures (**1**, **1BH-H**, **1BF-H**, **1BC-H**, **1BO-H**) were identified through the IRC of the proton transfer transition states and do not necessarily represent global minima. Final reaction energies arise from the summation of energies of the isolated structures. Geometric parameters of important atoms for starting structures and transition states can be found in Table S1 and those computed structures are assembled in Fig. 2.

Gibbs free energies, enthalpies and entropies for the proton-based elimination reaction for compounds **1**, **1BH-H**, **1BF-H**, **1BC-H**, and **1BO-H** can be found in Table 1. The Gibbs free energy of activation tracks with the enthalpy of activation, though a minor contribution is noted from the slight decrease in entropy of activation, which is most pronounced for the boron substituted sulfoxides. The introduction of a geminal boron species reduces the free energy barrier for sulfenic acid elimination by 6.2–15.8 kcal mol^{-1} compared to the unsubstituted sulfoxide **1** ($\Delta G^{\ddagger}$ = 34.3 kcal mol^{-1}). The trends roughly parallel the computed hydride affinities of the simplified series of compounds: BH_3 > $BHMe_2$ > BHF_2 > $BH(OH)_2$ (linear regression R^2 = 0.913).[52]

Table 1 Thermodynamics of methanesulfenic acid elimination from compounds **1** and **1B** [a]

Compound→	**1**	**1BH-H**	**1BF-H**	**1BC-H**	**1BO-H**
$\Delta H^{\ddagger}$	34	17.4	23.3	22.3	27.3
$\Delta G^{\ddagger}$	34.3	18.5	24.4	23.3	28.1
$\Delta S^{\ddagger}$	−1	−3.7	−3.7	−2.7	−2.7
ΔH	19.2	14.8	16	16.2	17.2
ΔG	7.5	2.3	3.8	3.6	4.1
ΔS	39	42	41	42.3	44.1

[a] Energy units are kcal mol^{-1}; entropy units are cal K^{-1} mol^{-1}.

Natural resonance theory (NRT) bond orders[45] for starting materials, transition states and products are compared in Table S2. Transition state values for compound **1**‡ are relatively balanced with regards to bond formation and breakage; S–C_α, C_β–H and O–H bond orders are 0.43, 0.49 and 0.46, respectively. Substitution of the boron functionality geminal to the proton transferred leads to asynchronicity of the reaction in the transition state: S–C_α and O–H bond orders in each of **1BH-H**‡, **1BC-H**‡, **1BF-H**‡, and **1BO-H**‡ are higher than **1**‡, indicating reduced S–C_α cleavage and advanced O–H bond formation, respectively, while the C_β–H bond order of the boron containing systems reveals advanced bond breakage compared to **1**‡, an effect that is most pronounced for compounds **1BH-H**‡ and **1BC-H**‡. Overall, it appears the boron functionality lowers barriers for sulfenic acid elimination by advancing aspects of bond formation and cleavage of the bonds directly involved in proton transfer.

Differences in these structural parameters and bond orders show that boron substitution has the greatest effect in the transition state, enhancing proton transfer while minimizing S–C_α bond breakage. NPA charges (Table S2) show an increased negative charge on the boron bearing carbon (C_β) of the boron substituted sulfoxides, compared to compound **1**. The increase in charge at the C_β position upon moving to the transition states is comparable for compounds **1**, **1BF-H**, and **1BO-H** (an increase of 0.08). However, for compounds **1BH-H** and **1BC-H** less charge buildup occurs.

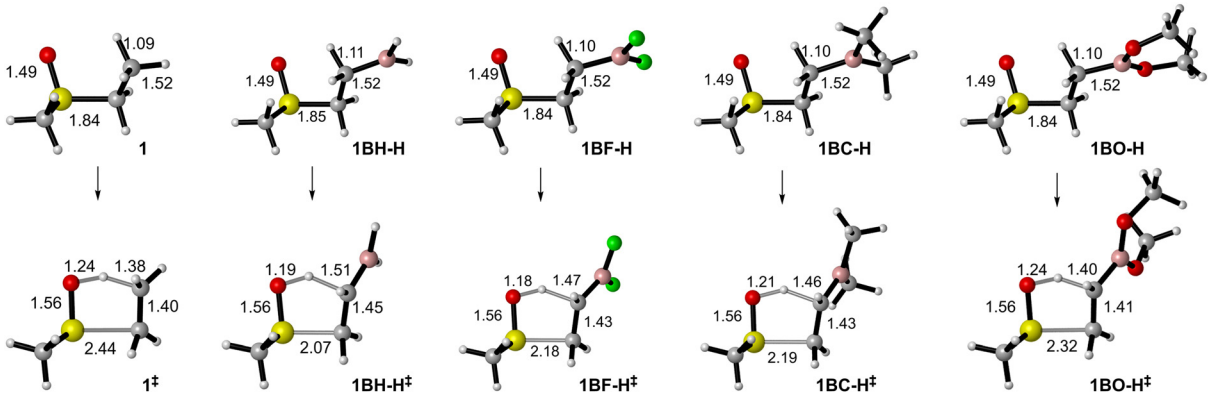

Fig. 2 Starting sulfoxides and transition states for the methanesulfenic acid elimination of sulfoxides **1** and **1B**. Bond lengths are listed in angstroms.

Open Access Article. Published on 05 January 2026. Downloaded on 1/11/2026 12:59:57 PM.
This article is licensed under a Creative Commons Attribution-NonCommercial 3.0 Unported Licence.

Compounds **1BH-H** and **1BC-H** also show a significant reduction in charge on the boron atom in the transition state (by 0.22 and 0.13, respectively) while the change for the more electronegative substituents is far less (by 0.06 and 0.02 for **1BF-H** and **1BO-H**, respectively), indicating the increased ability of the borane groups to accept density from C_β compared to their F and OMe counterparts. This repositioning of negative charge onto the β-carbon and the boron atom indicate stabilization of the charge development in the transition state is better managed when H or Me are attached to boron, leading to a more significant reduction in the free energy barrier. Delocalization and stabilization of charge can be identified and quantified through NBO second order perturbation theory in the NBO7 program.[46,53]

An examination of the most significant interactions in **1**‡ indicate the direct involvement of NBOs associated with proton transfer (bond formation and cleavage) and S–C_α cleavage; that is $n_O \rightarrow \sigma_{C_\beta-H}^*$ and $\sigma_{C_\beta-H} \rightarrow \sigma_{S-C_\alpha}^*$ provide stabilization energies of 114.4 kcal mol^{-1} and 35.9 kcal mol^{-1} respectively. These orbital interactions serve to promote both bond formation and breakage related to proton transfer, while also advancing S–C_α cleavage. The resulting synchronicity is reflected in the natural bond orders presented in Table S2. In contrast, in the ground states of **1BH-H**, **1BF-H**, **1BC-H** and **1BO-H** exhibit significant delocalization (14.19 kcal mol^{-1}, 9.57 kcal mol^{-1}, 11.30 kcal mol^{-1} and 9.00 kcal mol^{-1}, respectively) of density from $\sigma_{C_\beta-H}$ into the lone valence of boron is observed, weakening the bond prior to transition state formation. The extent of delocalization is reduced for boron substituents with donation capability of their own; the lone pairs of both fluorine and oxygen ligands in **1BF-H** and **1BO-H** donate significantly to the lone valence orbital on boron, with $n_{O/F} \rightarrow B_{(lv)}$ stabilization energies of 94.4 kcal mol^{-1} and 118.9 kcal mol^{-1}, respectively. The extent of donation is reflected further in transition states (**1BF-H**‡, **1BO-H**‡) in which the lone valence orbital of boron is no longer free but is instead occupied in π systems with O and F. Transition states with hydrogen and methyl substituents (**1BH-H**‡, **1BC-H**‡), however, still have a lone valence orbital on boron available to help stabilize charge redistribution.

It should be noted that the NBO program identifies more significant cleavage of the C_β–H bond such that a lone pair is present on C_β in both **1BF-H**‡ and **1BO-H**‡, which has been observed before by Kingsbury[12] upon fluorine substitution. The advanced nature of these transition states suggests the dominant interaction as that between the lone pair of C_β and the σ_{O-H}^* orbital, delaying bond formation behind cleavage – a concept well supported by the increased charge on C_β in both **1BF-H**‡ and **1BO-H**‡ (Table S2) and the higher barriers for proton transfer. However, both **1BH-H**‡ and **1BC-H**‡ still exhibit strong delocalization of the $\sigma_{C_\beta-H}$ orbital into the unoccupied boron lone valence orbital ($\sigma_{C_\beta-H} \rightarrow B_{(lv)}$). The left side of Fig. 3 shows the composite energy level diagram for the Ei reaction of compound family **1B** and ethyl methyl sulfoxide (**1**). Non-parenthesized $\Delta G^\ddagger$ values permit direct comparison of the borylated compounds.

Boryl sulfenate elimination from β-boryl sulfoxides

To assess the competition between hydrogen elimination and borane/boronate elimination, two sets of transition states for boryl sulfenate elimination from compounds **1B** were located. They were classified based on ring enveloping that placed a pseudoaxial boron substituent either *syn* or *anti* to the sulfur methyl group. The *anti* set of transition structures were either

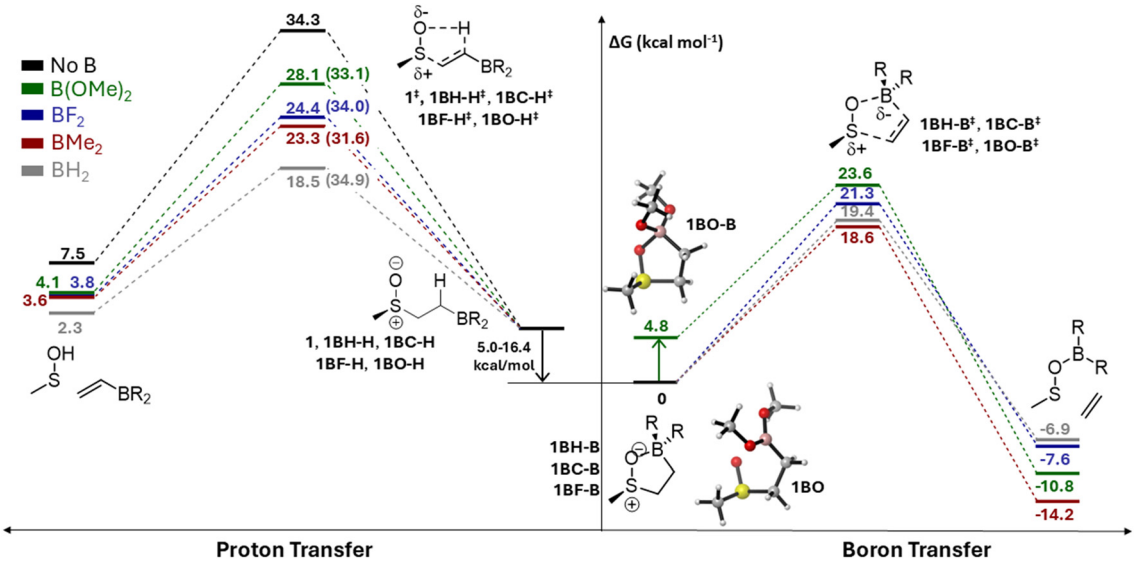

Fig. 3 Composite energy level diagram for sulfenic acid (left) and boryl sulfenate (right) eliminations of β-boro sulfoxides. Non-parenthesized values in the proton transfer manifold represented free energy barriers from local minima (**1**, **1BH-H**, **1BC-H**, **1BF-H**, **1BO-H**) for sulfenic acid elimination and the positional energy levels reflect these values. Parenthesized energy values in the proton transfer manifold are the $\Delta G^\ddagger$ barriers from the 0.0 kcal mol^{-1} position for compounds **1BH-B**, **1BC-B**, **1BF-B** and **1BO**.

Open Access Article. Published on 05 January 2026. Downloaded on 1/11/2026 12:59:57 PM.
This article is licensed under a Creative Commons Attribution-NonCommercial 3.0 Unported Licence.

of lower energy (−2.2 kcal mol^{-1} for BMe_2 group) or of comparable energies (within ±0.5 kcal mol^{-1}) compared to the *syn* structures. For reasons of simplicity and because a unified set of comparable geometries will permit a rational assessment of other parameters including role of boron substituents, the *anti*-transition states were adopted for study herein. Images of the *syn* transition states comprise Fig. S1.

Precursor compounds of this series were identified by further optimization of IRC-derived starting structures and through optimization of open-form structures and various precoordinated arrangements, the latter assessment addressing enveloping preferences of the B atom in relation to sulfur's methyl substituent. This process provided precoordinated structures **1BH-B**, **1BF-B** and **1BC-B** as minima for the $-BH_2$, $-BF_2$, and $-BMe_2$ substituted structures of lower free energy (16.4 kcal mol^{-1}, 9.6 kcal mol^{-1} and 8.3 kcal mol^{-1}, respectively) with an envelope shape. Precomplexed form **1BO-B** proved to be a local minimum as uncoordinated structure **1BO**, with no significant O → B interaction, was found to be 4.8 kcal mol^{-1} more stable. The implication is the sulfinyl oxygen is not a strong enough Lewis base to displace the internal coordination of the methoxy oxygens to boron's lone valence orbital.

Transition state geometries for **1BH-B**‡, **1BF-B**‡, **1BC-B**‡, **1BO-B**‡ can be found in Fig. 4. As with the ground-state molecules, transition states assume an envelope-like 5-membered ring with a tetracoordinate boron centre, in these cases, oriented *anti* to the sulfinyl methyl (Fig. 4). The S–C_α bond lengths are more extended in the boron group transfer transition states. Extension of the C_β–B bond is generally greater than the decreased distance between boron and the sulfinyl oxygen, excluding the case of **1BO**, where the lack of precoordination accounts for the significant change observed (Table S3).

The magnitudes of the free energy barriers for elimination boryl sulfenate are reduced by 3.1–9.3 kcal mol^{-1} compared to the parallel sulfenic acid elimination in all cases except **1BH-B** where $\Delta G^{\ddagger}$ increases from 18.5 to 19.4 kcal mol^{-1} (Table 2). As with the proton transfer, the barrier is principally enthalpic. Referencing both processes to a common global zero (Fig. 3, 0.0 kcal mol^{-1}) and using the parenthesized $\Delta G^{\ddagger}$ values of the proton-transfer manifold for sulfenic acid elimination, the boryl sulfenate elimination pathway is favored by 9.5–15.5 kcal mol^{-1} ($\Delta\Delta G^{\ddagger}$ entries, Table 2).

The enthalpic barriers for boron elimination exhibit only small variation across the series, despite their differing boron Lewis acidities. Natural steric analysis reveals a large increase in the total steric exchange (SXE) energy moving from **1BO** to **1BO-B**‡ of +46.4 kcal mol^{-1} as the structure tightens upon dative coordination of the sulfinyl oxygen to the boronate. For **1BO-B**, total steric exchange energy shows a slight decrease upon moving to the transition state by 1.1 kcal mol^{-1} as bond lengths elongate. Examination of the NPA charges for the starting sulfoxides, transition states and products in Table S4

Table 2 Thermodynamics of boryl sulfenate elimination from compounds **1B** [a]

Compound→	**1BH-B**	**1BF-B**	**1BC-B**	**1BO** [b]
$\Delta H^{\ddagger}$	19.4	21.8	18.9	23.1
$\Delta G^{\ddagger}$	19.4	21.3	18.6	23.6
$\Delta S^{\ddagger}$	0.0	1.7	0.9	−1.7
ΔH	6.8	7.1	0.4	2.6
ΔG	−6.9	−7.6	−14.2	−10.8
ΔS	45.8	49.3	49.0	45.0
$\Delta G^{\ddagger}$ MeSOH elim[c]	34.9	34.0	31.6	33.7
$\Delta\Delta G^{\ddagger}$[d]	15.5	12.7	12.0	9.5

[a] Energy units are kcal mol^{-1}; entropy units are cal K^{-1} mol^{-1}. [b] **1BO-B** is a stationary point on the path of **1BO** to the transition state. [c] Free energy difference for sulfenic acid elimination from lowest energy conformation. [d] Free energy difference between boryl sulfenate and sulfenic acid elimination from common lowest energy conformation.

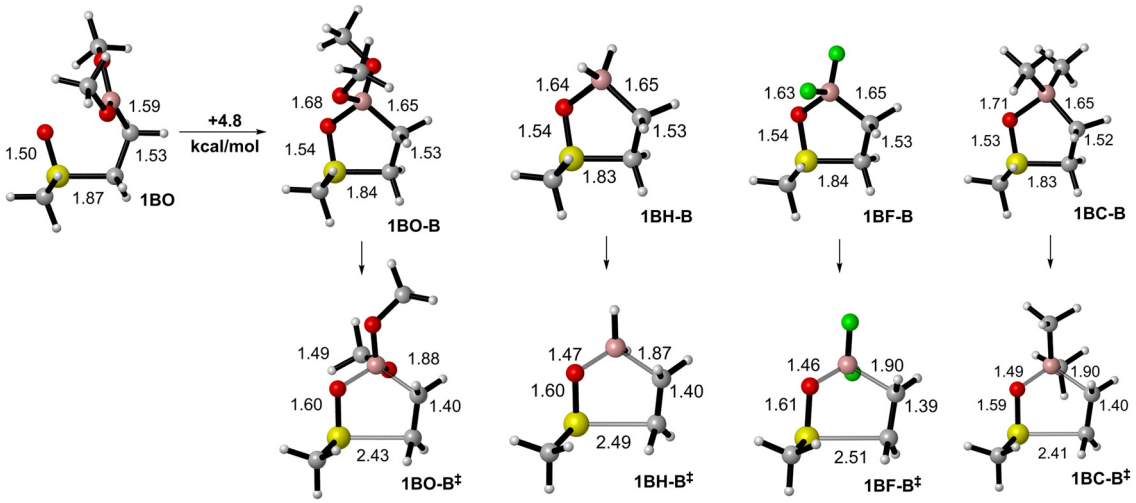

Fig. 4 Starting sulfoxides and transition states for the boryl sulfenate elimination of sulfoxides **1B**. Bond lengths are listed in angstroms.

Open Access Article. Published on 05 January 2026. Downloaded on 1/11/2026 12:59:57 PM.
This article is licensed under a Creative Commons Attribution-NonCommercial 3.0 Unported Licence.

reveals that charge in the transition state decreases significantly on C_α and slightly on C_β, contrary to the proton transfer reactions wherein charge on C_β increases marginally. The sulfur assumes an increasing negative charge in the transition states as it accepts electrons from C_α, while boron becomes more positive in all cases where pre-coordination has occurred.

The significant changes in charge on both sulfur and C_α correlate with a reduced transition state S–C_α bond order, indicating more advanced cleavage in the transition state for boron transfer. Both methyl and hydrogen substituted boranes have significantly higher O–B bond orders than their more electronegative counterparts. In terms of synchronicity, the changes in bond order in moving from the starting sulfoxide to the transition state (ΔBO) are most uniform for **1BH-B** and **1BC-B**. To understand the retardation of O–B bond formation in **1BF-B**‡ and **1BO-B**‡, second-order perturbation theory analysis was performed. The strongest interaction of the σ^*_{O-B} orbital is by the lone pairs of the methoxy oxygen and fluorine (13.09 and 11.66 kcal mol^{-1}, respectively), inhibiting bond formation. Additional details and graphics addressing differences in bond order for these compounds may be found in the SI (p. S6).

Conjugation effects on boron transfer

To determine the role of conjugation on the energetics of boron transfer three additional compound families were investigated, all possessing the H, F, Me and OMe boron substituents: **2B** with a vinyl sulfoxide, **3B** with a phenyl sulfoxide, and **4B** still with a methyl sulfoxide, but harbouring an alkene between the sulfur and boron atoms which leads to alkyne formation upon boryl sulfenate loss (Fig. 5). Some summary content of this part of the investigation is provided here; detailed outcomes, explanations and associated graphics and tables are found in the SI (pp. S7–S13, Tables S6–S8 and Fig. S3–S5).

Paralleling compounds **1B**, the sulfinyl to boron coordinated structures **2B**/**3B** with H, F and Me groups proved to be the lowest energy identified structures. Whereas for methoxy groups on the boron, the structures lacking significant oxygen to boron interaction (**2BO**/**3BO**) prevailed as global minima, lying 4.5 kcal mol^{-1} and 1.7 kcal mol^{-1} lower than coordinated local minima **2BO-B** and **3BO-B**, respectively. For compounds **2B**/**3B**, Gibbs energies of the boryl sulfenate elimination are generally reduced by 2.1–2.6 kcal mol^{-1}, with the **3BO** reaction as an outlier at 5.9 kcal mol^{-1}. These lower barriers are partially attributed to delocalization of the electron density in the S–C_α bond into the π* orbitals of the phenyl and vinyl groups (NBO analysis).

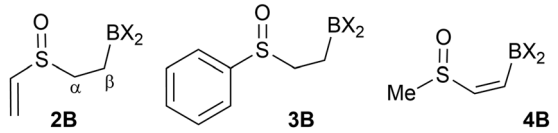

Fig. 5 Conjugated boryl sulfoxides under study (X = H, F, Me, OMe).

Regarding the sulfenyl borylate elimination of compounds **4B** free energy barriers for the elimination are increased significantly compared to **1B**, with free energy barriers increasing by 12.6–15.9 kcal mol^{-1} for the lowest energy starting sulfoxide starting structures. This observation is consistent with past work[13] and is to be expected as bond strengths of the C_β–B and C_α–S bonds should be increased due to the sp^2 character of the carbons involved.

Boronic esters – proton and boron transfer

Whereas the elimination chemistry of **1B-O** serves as an example of a boronic ester, particularly for comparison to other compounds **1B**, methoxy groups do not embody common boronate usage in organic chemistry. Accordingly,

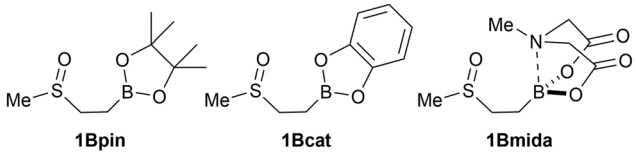

Fig. 6 Structures of boronate esters under study.

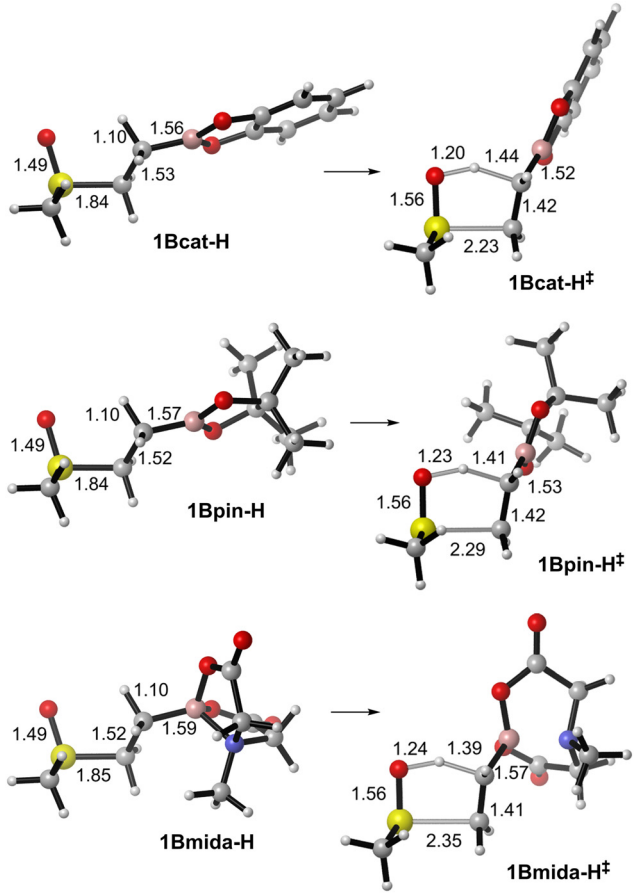

Fig. 7 Starting sulfoxides and transition states for the elimination of methanesulfenic acid from boronic ester substituted sulfoxides. Bond lengths are listed in angstroms.

Open Access Article. Published on 05 January 2026. Downloaded on 1/11/2026 12:59:57 PM.
This article is licensed under a Creative Commons Attribution-NonCommercial 3.0 Unported Licence.

the proton and boron transfer pathways for more popular boronates[54] were investigated. This section addresses compounds **1** featuring the more common boro-catechol (**1Bcat**), boro-pinacol (**1Bpin**) and boro-*N*-methyliminodiacetyl (**1Bmida**) esters[55,56] (Fig. 6). The latter are of particular interest since the normally trivalent boron is 'protected' through internal N → B coordination of the proximal nitrogen, which imparts additional stability to the substrate.[57]

Starting sulfoxide structures **1Bcat-H** and **1Bpin-H** were created from structure **1BO-H**, then resubmitted for further optimization. In the case of the BMIDA group, the global minimum was obtained by conformational sampling using the ORCA GOAT computational package; the 8 low energy structures obtained from that exercise were then optimized to afford **1Bmida**, possessing the nitrogen–boron bond approximately *anti* to one C_β–H bond. QTAIM and NBCP analysis confirm the presence of two interactions between hydrogens of the BMIDA group and the sulfinyl oxygen (Fig. S6). A reorientation of the $MeS(O)CH_2CH_2$ chain requires 6.8 kcal mol^{-1} and provides **1Bmida-H** a local minimum aligned for sulfenic acid elimination (Fig. 8).[55]

Table 3 Thermodynamics of sulfenic acid elimination from boronic esters **1B**[a]

Compound→	**1BO-H**	**1Bcat-H**	**1Bpin-H**	**1Bmida-H**
$\Delta H^\ddagger$	27.3	25.6	26.7	27.3
$\Delta G^\ddagger$	28.1	26.5	27.4	27.5
$\Delta S^\ddagger$	−2.7	−3.1	−2.5	−0.6
ΔH	17.2	16.6	17.2	15.0
ΔG	4.1	4.4	4.9	2.1
ΔS	44.1	41.0	41.3	43.2

[a] Energy units are kcal mol^{-1}; entropy units are cal K^{-1} mol^{-1}.

Transition states were located for the boronate esters, as shown in Fig. 7. Free energy barriers for methanesulfenic acid elimination and other thermodynamic parameters can be found in Table 3. The data for the **1BO-H** is provided for comparison.

As with **1BO-H**, stabilization in the reaction is found in ground state molecules **1Bpin-H** and **1Bcat-H** *via* delocalization of the C_β–H electron density into boron's lone valence in the ground state sulfoxides on the order of 9.37 kcal mol^{-1} and 9.67 kcal mol^{-1}, respectively. The free energies of activation for **1BO-H**‡ and **1Bpin-H**‡ are comparable and are ~1.7 kcal mol^{-1} greater than for **1Bcat-H**‡ (Table 3). In the corresponding transition states, a lone pair identified on C_β in **1Bpin-H**‡ donates into the π_{O-B}^* system with a stabilization energy of 53.37 kcal mol^{-1}, while in **1Bcat-H**‡ the C_β–H bonding orbital remains available to donate into the lone valence of boron with a stabilization energy of 36.64 kcal mol^{-1}.

Of particular interest is the lack of π systems between boron and oxygen within the catechol system, as analysed by the NBO program. The higher stabilization energy for **1Bpin-H**‡ is consistent with the localization of the electrons as a lone pair on C_β. Bond orders for the reaction for both the **Bpin** and **Bcat** systems show incredible similarities (Table S9) though slight differences are observed in the S–C_α, C_α–C_β and C_β–H bond orders in the transition states. In particular, addressing the **Bcat** system, the C_β–H bond is slightly weaker and C_α–C_β π-bond formation lags slightly. The larger increase in bond order of the C_β–B bond in **1Bcat-H**‡ does indicate a more significant role in engaging with the electron density on C_β.

Regarding **1Bmida-H**‡, the bond orders of C_β–H and O–H are almost equivalent meaning each has progressed exactly 50% of the way through its transition required for the elimination (Table S9). Additional delocalizations were identified in

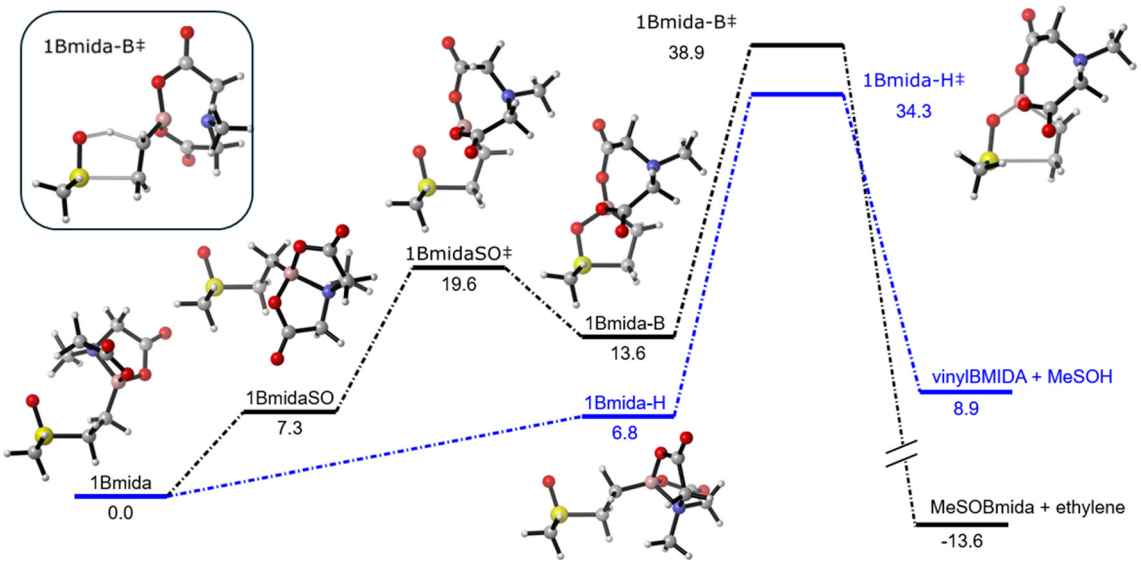

Fig. 8 Competitive elimination pathways for **1Bmida**.

Open Access Article. Published on 05 January 2026. Downloaded on 1/11/2026 12:59:57 PM.
This article is licensed under a Creative Commons Attribution-NonCommercial 3.0 Unported Licence.

Table 4 Thermodynamics of boryl sulfenate elimination from boronic esters **1B** [a]

Compound→	**1BO** [b]	**1Bpin**	**1Bcat-B**	**1Bmida** [c]
$\Delta H^{\ddagger}$	23.1	23.5	22.3	40.5
$\Delta G^{\ddagger}$	23.6	24.5	21.8	38.9
$\Delta S^{\ddagger}$	−1.7	−3.1	1.6	5.4
ΔH	2.6	−1.3	2.2	−1.1
ΔG	−10.8	−13.4	−11.3	−13.6
ΔS	45.0	40.7	45.4	41.9
$\Delta G^{\ddagger}$ MeSOH elim [d]	33.1	28.2	28.5	34.3
$\Delta\Delta G^{\ddagger}$ [e]	9.5	3.7	6.7	−4.6

[a] Energy units are kcal mol^{-1}; entropy units are cal K^{-1} mol^{-1}. [b] **1BO-B** is a stationary point on the path of **1BO** to the transition state. [c] **1Bmida-B**‡ is one of several stationary points on the path of **1Bmida** to the transition state. [d] Free energy difference for sulfenic acid elimination from lowest energy conformation. [e] Free energy difference between boryl sulfenate and sulfenic acid elimination from common lowest energy conformation.

the transition state as the alignment of the B–N bond of the BMIDA group was found to be 176° with respect to the C_{β}–H bond allowing donation into the σ_{B-N}^{*} and antibonding orbital. The stabilization energy for this interaction is 14.12 kcal mol^{-1}.

For boryl sulfenate elimination, we were able to locate suitable ground state and transition state structures for the **Bpin** and **Bcat** containing structures. The lowest energy structure, **1Bpin**, exhibits the sulfinyl oxygen near the boronate, yet the boron remains trivalent as with structure **1BO**. We were unable to locate a converged structure with a sulfinyl oxygen coordinated to the B, analogous to **1BO-B**, and **1Bpin** was found to lead to **1Bpin-B**‡ (IRC). On the other hand, minima **1Bcat** and **1Bcat-B** were both located, with the latter residing 1.8 kcal mol^{-1} lower, and remaining on the PES leading to **1Bcat-B**‡ (Fig. 9). This observation contrasts with the other boronic esters investigated in this study. The free energy barrier for elimination of boron in **1Bpin** leads to a barrier 0.9 kcal mol^{-1} higher than was observed for compound **1BO** (23.6 kcal mol^{-1}), while the **Bcat** derivative has a decrease of 1.8 kcal mol^{-1} (Table 4). Referring to the competitive thermal elimination options, boryl sulfenate loss remains preferred. However, the $\Delta\Delta G^{\ddagger}$ values of 3.7 (**1Bpin**) and 6.7 kcal mol^{-1} (**1Bcat**) are reduced compared to the $\Delta\Delta G^{\ddagger}$ of 9.5 kcal mol^{-1} for **1BO**. A composite table of thermodynamic parameters comparing all reactions can be found in the SI (Table S11).

For the **Bcat** and **Bpin** systems only minor differences in the bond orders are noted (Table S10). Comparing **1Bcat** and **1Bpin**, both of which leave the boron as tricoordinate, the S–C_{α} bond order in **1Bcat** is slightly weaker, while the C_{α}–C_{β} bond is slightly stronger than **1Bpin**. Coordination of the boron to the sulfinyl oxygen reduces the strength of the C_{α}–C_{β} bond but increases the strength of the S–C_{α} bond. Transition states for both the **Bcat** and **Bpin** families are similar, but the strength of the O–B interaction is greatest in **1Bcat-B**‡.

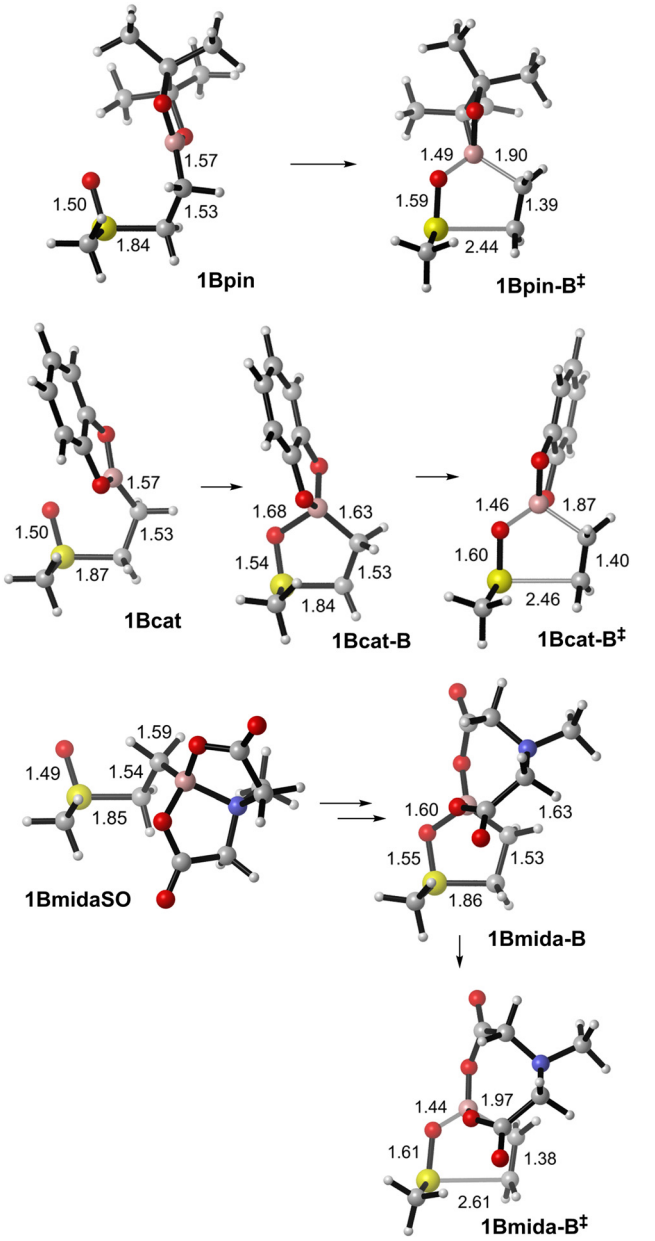

Fig. 9 Structures and pathways for the boryl sulfenate elimination of **BCat**, **BPin** and **Bmida** boronic esters. Bond lengths are listed in angstroms.

The BMIDA group introduces a different option for consideration when assessing the sulfenyl boronate elimination. The sulfinyl oxygen is able to achieve back-side displacement[58] of the coordinating nitrogen, consistent with the intramolecular actions of a nitrone oxygen on the BMIDA group.[59] Indeed after reorientation of **1Bmida** to local minimum **1BmidaSO**, a validated transition state for backside displacement was found (**1BmidaSO**‡). The overall barrier of 19.6 kcal mol^{-1} remains less than the simple release of the coordinating nitrogen from the boron which results in a species ~27–31 kcal mol^{-1} higher in energy.[58]

Open Access Article. Published on 05 January 2026. Downloaded on 1/11/2026 12:59:57 PM.
This article is licensed under a Creative Commons Attribution-NonCommercial 3.0 Unported Licence.

Through the nitrogen displacement transition state, structure **1Bmida-B** is obtained, which is primed for boryl sulfenate elimination, a process that proceeds through **1Bmida-B**‡ with a barrier of 25.3 kcal mol^{-1}. Transition state **1Bmida-B**‡ exhibits a O–B interaction that is significantly advanced compared to **1Bpin-B**‡ and **1Bcat-B**‡. The thermodynamic values for the boronate ester based elimination options can be found in Table 4 and selected structures and parameters are shown in Fig. 9. Effects of the boronic ester on the synchronicity of the elimination reactions can be drawn from changes in bond order, found in Table S10.

Given the ground state nature of the BMIDA group, and the 19.6 kcal mol^{-1} energy requirement to access an SO → B species, and the higher barrier for eventual elimination, this system presents the highest barrier for boryl sulfenate elimination. Indeed, the BMIDA substituted sulfoxide shows a 4.6 kcal mol^{-1} preference for the hydrogen elimination reaction over the elimination involving the BMIDA group itself (Fig. 8) Given the preferred Ei pathway for this BMIDA substrate and the similarity of the $\Delta G^{\ddagger}$ values of 33.1 kcal mol^{-1} for **1Bmida-H**‡ to 34.3 kcal mol^{-1} for **1**‡, one can conclude the substituent influence of the BMIDA group on the Ei of methanesulfenic acid is marginal.

Conclusions

Through gas phase computational analysis with a focus on the electronics of the system, the effect of the addition of a boron-based substituent to the C_β position on the barriers for the classic Ei reaction of sulfoxides was assessed. Sulfenic acid elimination benefited from lower Gibbs energies of activation and enthalpy of activation[13] due to the ability of the boron functionality to accept electron density of the C_β–H bond. The addition of any boron group leads to asynchronicity in the transition state by advancing both C_β–H bond cleavage and O–H bond formation by stabilization of the enhanced electron density on C_β. This also leads to reduced cleavage of the S–C_α bond relative to the transition state for ethyl methyl sulfoxide.

However, compounds **1B** prefer lower energy local minima that correlate to boryl sulfenate elimination (Fig. 3). Gibbs energies of activation for this process are 9.5–15.5 kcal mol^{-1} lower than the corresponding proton transfer reactions, meaning boryl sulfenate elimination is predicted in every instance. Our predicted trends follow past work for the Ei chemistry of selenoxides,[34] although as expected in a comparison of the two chalcogens, the sulfur barriers are higher.

The effect of conjugation on the sulfur or the alkyl portion of the sulfoxide was investigated through compound families **2B**, **3B**, and **4B**. Reduced Gibbs energies of activation of 1.9–4.9 kcal mol^{-1} for compound families **2B** and **3B** relative to compound family **1B** were attributed to greater stabilization of charge development on sulfur in the transition state through delocalization into the vinyl or phenyl system, as verified by NPA charges and second-order perturbation energies. Conjugation between sulfur and the boron functionality was explored through compound family **4B**. Gibbs energies of activation were higher than family **1B** by 12.6–15.9 kcal mol^{-1} as expected for elimination from an sp^2 hybridized carbon.

A comparison of the effects of common boronic esters employed catechol and pinacol derived esters, as well as BMIDA. Both proton transfer and boronic ester reaction pathways were modelled. The Gibbs energies of activation for the proton transfer reaction were similar to those of **1BO-H**, with the $\Delta G^{\ddagger}$ for the **Bcat** system resting 1.6 kcal mol^{-1} lower. For boronic ester transfer, the **Bcat** system again displayed slightly lower Gibbs energies of activation. The BMIDA substituted sulfoxide proved unique in that the methanesulfenic acid elimination was comparable to methyl ethyl sulfoxide and boryl sulfenate elimination is higher in energy due to the loss of N → B coordination of the BMIDA group.

Practical applications pursuant to work would benefit from the incorporation of solvent effects to the potential energy surfaces for more accurate relative free energy barriers. Nevertheless, this contribution guides synthetic chemistry in the management, design and synthetic value of compounds possessing boron functionality β to sulfoxides. Our data reveals the thermal *syn* elimination of sulfenic acid will only occur when the boron atom is part of the BMIDA assembly. The other boron containing structures are predicted to thermally eliminate boryl sulfenate in preference to sulfenic acid formation, offering an olefination protocol to the community.

Author contributions

E. A. N. contributed data curation, formal analysis, visualization, writing – original draft. A. L. S. contributed funding acquisition, supervision. Both authors contributed conceptualization, investigation, methodology, project administration, writing – review & editing.

Conflicts of interest

There are no conflicts to declare.

Data availability

Data generated and analysed during this study are provided in full within the published article and the supplementary information (SI). Supplementary information: additional graphics, tables of data, a full description of the boryl sulfenate elimination chemistry of **2B**/**3B**/**4B**, a summary of second order perturbation theory stabilization energies, *xyz* coordinates and thermochemistry of structures. See DOI: https://doi.org/10.1039/d5ob01455g.

Acknowledgements

The authors are grateful for the computational support and resources provided by the facilities of the Shared Hierarchical

Open Access Article. Published on 05 January 2026. Downloaded on 1/11/2026 12:59:57 PM.
This article is licensed under a Creative Commons Attribution-NonCommercial 3.0 Unported Licence.

Academic Research Computing Network (SHARCNET) and the Digital Research Alliance of Canada. The authors are indebted to the Natural Sciences and Engineering Research Council (NSERC) of Canada for generously funding this research (grant RGPIN-2020-04029).

References

1 B. M. Trost and T. N. Salzmann, *J. Am. Chem. Soc.*, 1973, **95**, 6840–6842.
2 C. A. Kingsbury and D. J. Cram, *J. Am. Chem. Soc.*, 1960, **82**, 1810–1819.
3 R. B. Morin, B. G. Jackson, R. A. Mueller, E. R. Lavagnino, W. B. Scanlon and S. L. Andrews, *J. Am. Chem. Soc.*, 1963, **85**, 1896–1897.
4 K. Hori, S. Kamo and K. Sugita, *Org. Biomol. Chem.*, 2022, **20**, 9138–9141.
5 J. Rautschek, A. Jäger and P. Metz, *Org. Lett.*, 2018, **20**, 832–835.
6 Y. Wang, W. Ju, H. Tian, W. Tian and J. Gui, *J. Am. Chem. Soc.*, 2018, **140**, 9413–9416.
7 S. Goswami, K. Harada, M. F. El-Mansy, R. Lingampally and R. G. Carter, *Angew. Chem., Int. Ed.*, 2018, **57**, 9117–9121.
8 M. C. Carreño, Á. Somoza, M. Ribagorda and A. Urbano, *Chem. – Eur. J.*, 2007, **13**, 879–890.
9 D. Kim, J. Do, K. Kim, Y. Kim, H. Lee, B. Seo, W. Lee, H. B. Jeon, H. Y. Cho and H.-j. Paik, *Macromolecules*, 2021, **54**, 7716–7723.
10 E. Kesters, S. Swier, G. Van Assche, L. Lutsen, D. Vanderzande and B. Van Mele, *Macromolecules*, 2006, **39**, 3194–3201.
11 A. Trachsel, S. Leocata, J.-Y. de Saint Laumer and A. Herrmann, *Helv. Chim. Acta*, 2024, **107**, e202400046.
12 C. A. Kingsbury, *J. Phys. Org. Chem.*, 2010, **23**, 513–518.
13 J. W. Cubbage, Y. Guo, R. D. McCulla and W. S. Jenks, *J. Org. Chem.*, 2001, **66**, 8722–8736.
14 C. M. A. Gangemi, E. D'Agostino, M. C. Aversa, A. Barattucci and P. M. Bonaccorsi, *Tetrahedron*, 2023, **143**, 133550.
15 A. Barattucci, M. C. Aversa, A. Mancuso, T. M. G. Salerno and P. Bonaccorsi, *Molecules*, 2018, **23**, 1030.
16 P. M. Bonaccorsi, C. M. A. Gangemi, M. Monforte, E. D'Agostino and A. Barattucci, *ARKIVOC*, 2024, 202412256.
17 D. W. Emerson, A. P. Craig and I. W. Potts Jr., *J. Org. Chem.*, 1967, **32**, 102–105.
18 T. Yoshimura, E. Tsukurimichi, Y. Iizuka, H. Mizuno, H. Isaji and C. Shimasaki, *Bull. Chem. Soc. Jpn.*, 2006, **62**, 1891–1899.
19 B. S. Jursic, *J. Mol. Struct.: THEOCHEM*, 1997, **389**, 257–263.
20 L. Claes, J.-P. François and M. S. Deleuze, *J. Am. Chem. Soc.*, 2002, **124**, 7563–7572.
21 M. C. Aversa, A. Barattucci, P. Bonaccorsi and A. Contini, *J. Phys. Org. Chem.*, 2009, **22**, 1048–1057.
22 A. Madabeni, S. Zucchelli, P. A. Nogara, J. B. T. Rocha and L. Orian, *J. Org. Chem.*, 2022, **87**, 11766–11775.
23 H. J. Reich, I. L. Reich and J. M. Renga, *J. Am. Chem. Soc.*, 1973, **95**, 5813–5815.
24 K. B. Sharpless and R. F. Lauer, *J. Am. Chem. Soc.*, 1973, **95**, 2697–2699.
25 A. Madabeni, M. Bortoli, P. A. Nogara, G. Ribaudo, M. Dalla Tiezza, L. Flohé, J. B. T. Rocha and L. Orian, *Chem. – Eur. J.*, 2024, **30**, e202403003.
26 A. G. Davies, *J. Chem. Soc., Perkin Trans. 1*, 2000, 1997–2010.
27 M. Ochisi, S.-i. Tada, K. Sumi and E. Fujita, *J. Chem. Soc., Chem. Commun.*, 1982, 281–282.
28 I. Fleming and D. A. Perry, *Tetrahedron Lett.*, 1981, **22**, 5095–5096.
29 I. Fleming, J. Goldhill and D. A. Parry, *J. Chem. Soc., Perkin Trans. 1*, 1982, 1563–1569.
30 S. Nakamura, S. Kusuda, K. Kawamura and T. Toru, *J. Org. Chem.*, 2002, **67**, 640–647.
31 R. D. McCulla and W. S. Jenks, *J. Org. Chem.*, 2003, **68**, 7871–7879.
32 A. G. Durant, E. A. Nicol, B. M. McInnes and A. L. Schwan, *Org. Biomol. Chem.*, 2022, **20**, 649–657.
33 R. J. Armstrong, M. Nandakumar, R. M. P. Dias, A. Noble, E. L. Myers and V. K. Aggarwal, *Angew. Chem., Int. Ed.*, 2018, **57**, 8203–8208.
34 R. J. Armstrong, C. García-Ruiz, E. L. Myers and V. K. Aggarwal, *Angew. Chem., Int. Ed.*, 2017, **56**, 786–790.
35 C. Lee, W. Yang and R. G. Parr, *Phys. Rev. B: Condens. Matter Mater. Phys.*, 1988, **37**, 785–789.
36 B. Miehlich, A. Savin, H. Stoll and H. Preuss, *Chem. Phys. Lett.*, 1989, **157**, 200–206.
37 A. D. Becke, *J. Chem. Phys.*, 1993, **98**, 5648–5652.
38 S. Grimme, J. Antony, S. Ehrlich and H. Krieg, *J. Chem. Phys.*, 2010, **132**, 154104.
39 F. Weigend and R. Ahlrichs, *Phys. Chem. Chem. Phys.*, 2005, **7**, 3297–3305.
40 M. J. Frisch, G. W. Trucks, H. B. Schlegel, G. E. Scuseria, M. A. Robb, J. R. Cheeseman, G. Scalmani, V. Barone, G. A. Petersson, H. Nakatsuji, X. Li, M. Caricato, A. V. Marenich, J. Bloino, B. G. Janesko, R. Gomperts, B. Mennucci, H. P. Hratchian, J. V. Ortiz, A. F. Izmaylov, J. L. Sonnenberg, D. Williams-Young, F. Ding, F. Lipparini, F. Egidi, J. Goings, B. Peng, A. Petrone, T. Henderson, D. Ranasinghe, V. G. Zakrzewski, J. Gao, N. Rega, G. Zheng, W. Liang, M. Hada, M. Ehara, K. Toyota, R. Fukuda, J. Hasegawa, M. Ishida, T. Nakajima, Y. Honda, O. Kitao, H. Nakai, T. Vreven, K. Throssell, J. A. Montgomery Jr., J. E. Peralta, F. Ogliaro, M. J. Bearpark, J. J. Heyd, E. N. Brothers, K. N. Kudin, V. N. Staroverov, T. A. Keith, R. Kobayashi, J. Normand, K. Raghavachari, A. P. Rendell, J. C. Burant, S. S. Iyengar, J. Tomasi, M. Cossi, J. M. Millam, M. Klene, C. Adamo, R. Cammi, J. W. Ochterski, R. L. Martin, K. Morokuma, O. Farkas,

Open Access Article. Published on 05 January 2026. Downloaded on 1/11/2026 12:59:57 PM.
This article is licensed under a Creative Commons Attribution-NonCommercial 3.0 Unported Licence.

J. B. Foresman and D. J. Fox, *Gaussian 16, Revision C.01*, Gaussian, Inc., Wallingford CT, 2016.
41 C. Riplinger and F. Neese, *J. Chem. Phys.*, 2013, **138**, 034106.
42 C. Riplinger, P. Pinski, U. Becker, E. F. Valeev and F. Neese, *J. Chem. Phys.*, 2016, **144**, 024109.
43 F. Neese, *Wiley Interdiscip. Rev.: Comput. Mol. Sci.*, 2012, **2**, 73–78.
44 F. Neese, *Wiley Interdiscip. Rev.: Comput. Mol. Sci.*, 2018, **8**, e1327.
45 E. D. Glendening and F. Weinhold, 1998, **19**, 610–627.
46 E. D. Glendening, J. K. Badenhoop, A. E. Reed, J. E. Carpenter, J. A. Bohmann, C. M. Morales, P. Karafiloglou, C. R. Landis and F. Weinhold, *NBO 7.0*, University of Wisconsin, 2018.
47 J. K. Badenhoop and F. Weinhold, *J. Chem. Phys.*, 1997, **107**, 5406–5421.
48 F. Biegler-König and J. Schönbohm, *J. Comput. Chem.*, 2002, **23**, 1489–1494.
49 F. Neese, *Wiley Interdiscip. Rev.: Comput. Mol. Sci.*, 2025, **15**, e70019.
50 B. de Souza, *Angew. Chem., Int. Ed.*, 2025, **64**, e202500393.
51 C. Y. Legault, *CYLview, 1.0b*, Université de Sherbrooke, 2009, (https://www.cylview.org).
52 R. Vianello and Z. B. Maksić, *Inorg. Chem.*, 2005, **44**, 1095–1102.
53 F. L. Weinhold and C. R. Landis, *Discovering Chemistry with Natural Bond Orbitals*, John Wiley & Sons, Inc., 2012.
54 D. G. Hall, in *Boronic Acids*, ed. D. G. Hall, Wiley-VCH Verlag, 2011, ch. 1, DOI: 10.1002/9783527639328.ch1.
55 T. Mancilla, R. Contreras and B. Wrackmeyer, *J. Organomet. Chem.*, 1986, **307**, 1–6.
56 E. P. Gillis and M. D. Burke, *J. Am. Chem. Soc.*, 2007, **129**, 6716–6717.
57 A. Trofimova, B. White, D. B. Diaz, M. J. Širvinskas, A. Lough, T. Dudding and A. K. Yudin, *Angew. Chem., Int. Ed.*, 2024, **63**, e202319842.
58 J. A. Gonzalez, O. M. Ogba, G. F. Morehouse, N. Rosson, K. N. Houk, A. G. Leach, P. H. Y. Cheong, M. D. Burke and G. C. Lloyd-Jones, *Nat. Chem.*, 2016, **8**, 1067–1075.
59 C. F. Lee, D. B. Diaz, A. Holownia, S. J. Kaldas, S. K. Liew, G. E. Garrett, T. Dudding and A. K. Yudin, *Nat. Chem.*, 2018, **10**, 1062–1070.